

SHEP 95-27, OUTP-95-31P

hep-ph/9508346

Non-Minimal Supersymmetric Higgs Bosons at LEP2

S. F. King¹ and P. L. White²

¹*Physics Department, University of Southampton,
Southampton, SO17 1BJ, UK.*

Email king@soton.ac.uk

and

²*Theoretical Physics, University of Oxford
1 Keble Road, Oxford OX1 3NP, UK.*

Email plw@thphys.ox.ac.uk

Abstract

We discuss the discovery reach of LEP2 for the Higgs sector of a general extension of the MSSM including a single gauge singlet field. This change introduces a new quartic Higgs boson self-coupling which can increase the masses of the CP-even states, and also allows mixing between singlet and non-singlet states which can reduce the couplings of the mass eigenstates to the Z . The lightest CP-even Higgs boson is bounded by a parameter Λ which takes a maximum value $\Lambda_{max} \approx 136 - 146$ GeV for top mass $150 - 195$ GeV. We generalise the discussion of the bound to include the entire CP-even spectrum and show how experiment may exclude values of Λ smaller than some Λ_{min} . CP-even Higgs boson searches at LEP2 will be able to exclude

$\Lambda_{min} \approx 81 - 105$ GeV, depending on the machine parameters. We also present exclusion plots in the $m_A - \tan\beta$ plane, based on an analysis of CP-even, CP-odd and charged Higgs production processes at LEP2.

1 Introduction

The minimal supersymmetric standard model (MSSM) [1] has a Higgs sector consisting of two doublets H_1 and H_2 coupling to the down-type quarks and charged leptons, and to the up-type quarks respectively. The particle content, other than Goldstone bosons, is then two CP-even states h , H ; one CP-odd state A ; and a charged scalar H^\pm . The requirements of supersymmetry and gauge invariance then constrain the quartic Higgs coupling in terms of the gauge couplings, and we are left with only two free parameters to describe the whole Higgs sector. These are conventionally taken to be m_A , the mass of the CP-odd state, and $\tan\beta = \nu_2/\nu_1$ where $\nu_i = \langle H_i^0 \rangle$, and $\nu_1^2 + \nu_2^2 = \nu^2 = (174\text{GeV})^2$. It is then straightforward to derive the formulae $m_h^2 \leq M_Z$ and $m_{H^\pm} \geq M_W$ where the first of these in particular is greatly affected by radiative corrections[2]. Thus the MSSM is quite constrained and leads to the usual LEP2 Higgs discovery limits in the $m_A - \tan\beta$ plane.

If the Higgs sector of the MSSM is extended by the addition of further particle content then much of this predictivity is lost. This occurs for two reasons. Firstly, the constraint on the quartic couplings in the Higgs sector is not purely a result of supersymmetry but also an artefact of having only doublets in the Higgs sector, making it impossible to introduce extra Yukawa couplings through the Higgs superpotential in a way consistent with gauge invariance. Increasing the particle content and including such Yukawa couplings destroys both the upper bound on m_h and the lower bound on m_{H^\pm} . Secondly, the extra states which we can introduce will mix with the states present in the MSSM, and can alter both their couplings and their masses.

For example, in the next-to-MSSM (NMSSM) where there is an extra gauge singlet state N which only couples through the Higgs superpotential, and where there are only trilinear terms in the superpotential [3], there are now three CP-even neutral Higgs scalars and two CP-odd neutral Higgs scalars, due to the real and imaginary

components of the additional singlet scalar. In this model the lightest CP-even neutral scalar may be significantly heavier than in the MSSM, and to make matters worse this lightest CP-even scalar may have diluted couplings to the Z boson due to the admixture of singlet component [3, 4]. However, it is possible to derive a bound on the lightest CP-even state, both in this and in more general models [5, 6, 4]. Furthermore, in the limit that the lightest CP-even Higgs boson is completely decoupled (and hence we might think that the bound does not tell us anything about states which could be detected), the bound applies instead to the second lightest CP-even Higgs boson, while for light states which are merely weakly coupled one can derive precise bounds on their heavier partners. These become closer to the bound on the lightest as the singlet component of the lightest becomes greater [7].

Our intention in this paper is to discuss how much of the parameter space of such a general SUSY model can be covered by searches at LEP2, comparing them closely with the corresponding results for the MSSM. We shall consider the most general possible model with a gauge singlet and show that LEP2 can discover CP-even Higgs states in any part of the $m_A - \tan\beta$ plane, and can exclude significant parts of this plane even with the most general possible mixing.

We begin with a short review of the MSSM and its simplest extensions and how they affect the mass matrices. In section 4, we discuss the conventional bound on the lightest CP-even state in this model. In section 5, a number of search strategies are discussed, and we consider how effective the various MSSM searches are in an extended model. Finally, in section 6 we present results applicable to LEP2. Section 7 is the conclusion.

2 The MSSM

Here the superpotential is:

$$W_{MSSM} = -\mu H_1 H_2 + \dots \quad (2.1)$$

where $H_1 H_2 = H_1^0 H_2^0 - H_1^- H_2^+$.

The superpotential leads to the tree-level Higgs potential:

$$\begin{aligned} V_{MSSM} &= m_1^2 |H_1|^2 + m_2^2 |H_2|^2 + m_{12}^2 (H_1 H_2 + H.c.) \\ &+ \frac{1}{8} (g^2 + g'^2) (|H_1|^2 - |H_2|^2)^2 + \frac{g^2}{2} |H_1^* H_2|^2 \end{aligned} \quad (2.2)$$

where $m_1^2 = m_{H_1}^2 + \mu^2$, $m_2^2 = m_{H_2}^2 + \mu^2$, and $m_{12}^2 = -B\mu$ where B and $m_{H_i}^2$ are the usual soft SUSY-breaking terms.

The tree-level CP-odd mass-squared matrix is

$$M_A^2 = \begin{pmatrix} m_{12}^2 t_\beta & m_{12}^2 \\ m_{12}^2 & m_{12}^2 / t_\beta \end{pmatrix} \quad (2.3)$$

M_A^2 is diagonalised by $U M_A^2 U^\dagger = \text{diag}(m_A^2, 0)$ where U is given by

$$U = \begin{pmatrix} s_\beta & c_\beta \\ -c_\beta & s_\beta \end{pmatrix} \quad (2.4)$$

and m_A is given by $m_A^2 = m_{12}^2 / (s_\beta c_\beta)$ where $s_\beta = \sin \beta$, $c_\beta = \cos \beta$ and $t_\beta = \tan \beta$.

The tree-level charged Higgs mass squared matrix is

$$M_{H^\pm}^2 = \begin{pmatrix} M_W^2 s_\beta^2 + m_{12}^2 t_\beta & M_W^2 s_\beta c_\beta + m_{12}^2 \\ M_W^2 s_\beta c_\beta + m_{12}^2 & M_W^2 c_\beta^2 + m_{12}^2 / t_\beta \end{pmatrix} \quad (2.5)$$

$M_{H^\pm}^2$ is diagonalised by $U M_{H^\pm}^2 U^\dagger = \text{diag}(m_{H^\pm}^2, 0)$ where U is as before and m_{H^\pm} is given by $m_{H^\pm}^2 = M_W^2 + m_A^2$.

The tree-level CP-even Higgs mass-squared matrix is, after substituting the tree-level expression for m_{12}^2 in terms of m_A^2 ,

$$M^2 = \begin{pmatrix} M_Z^2 c_\beta^2 + m_A^2 s_\beta^2 & -(M_Z^2 + m_A^2) s_\beta c_\beta \\ -(M_Z^2 + m_A^2) s_\beta c_\beta & M_Z^2 s_\beta^2 + m_A^2 c_\beta^2 \end{pmatrix} \quad (2.6)$$

M^2 is diagonalised by $VM^2V^\dagger = \text{diag}(m_H^2, m_h^2)$ where

$$V = \begin{pmatrix} c_\alpha & s_\alpha \\ -s_\alpha & c_\alpha \end{pmatrix} \quad (2.7)$$

where $-\pi/2 \leq \alpha \leq 0$ and m_h^2, m_H^2 are given by

$$m_{H,h}^2 = \frac{1}{2}(m_A^2 + M_Z^2) \pm \frac{1}{2}\sqrt{(m_A^2 + M_Z^2)^2 - 4m_A^2 M_Z^2 c_{2\beta}^2} \quad (2.8)$$

and the two angles are related by:

$$\tan 2\alpha = \tan 2\beta \frac{(m_A^2 + M_Z^2)}{(m_A^2 - M_Z^2)} \quad (2.9)$$

In the above conventions, the ZZh coupling has an additional factor of $\sin(\beta - \alpha)$ relative to the standard model, and the ZZH coupling has a factor of $\cos(\beta - \alpha)$. The ZhA coupling is proportional to $\cos(\beta - \alpha)$.

It is interesting to observe that if we do not diagonalise M^2 but instead rotate to a primed basis where the second Higgs doublet does not have any VEV, then the 11 element of the matrix no longer contains any m_A dependence. Since the smallest eigenvalue of a real symmetric matrix is less than or equal to the smallest diagonal term, this gives a useful upper bound on the lightest CP-even Higgs mass. This rotation is given by $WM^2W^\dagger = M'^2$ where

$$W = \begin{pmatrix} c_\beta & s_\beta \\ -s_\beta & c_\beta \end{pmatrix} \quad (2.10)$$

and the bound is then given by

$$m_h^2 \leq M_{11}'^2 = M_Z^2 \cos^2 2\beta. \quad (2.11)$$

Starting from the primed basis the CP-even Higgs matrix is diagonalised by

$$XM'^2X^\dagger = \text{diag}(m_H^2, m_h^2) \quad (2.12)$$

where $X = VW^\dagger$.

Note that in this basis the additional factor in the ZZh coupling relative to the standard model of $\sin(\beta - \alpha)$ is simply X_{21} , and similarly the ZZH factor of $\cos(\beta - \alpha)$ is just X_{11} .

3 The MSSM plus a Singlet

Now let us consider a very general Higgs superpotential of the form

$$W = W_{MSSM} + \lambda N H_1 H_2 + f(N) \quad (3.1)$$

where f is an arbitrary holomorphic function of N , the singlet field, and H_1 and H_2 are the usual Higgs doublets coupling to down and up quarks respectively. Since the singlet does not have gauge couplings we may then write

$$\begin{aligned} V = & V_{MSSM} + \lambda^2 |H_1 H_2|^2 \\ & + \left(\lambda(N + \bar{N})\mu + \lambda^2 |N|^2 \right) (|H_1|^2 + |H_2|^2) \\ & + \left(\lambda \frac{\partial \bar{f}}{\partial \bar{N}} - \lambda N A_\lambda \right) H_1 H_2 + h.c. + \dots \end{aligned} \quad (3.2)$$

where the ellipsis indicates terms with no dependence on H_1 or H_2 . Given that V_{MSSM} includes terms $\mu^2(|H_1|^2 + |H_2|^2)$ and $B\mu H_1 H_2$ it is then clear that we can account for the effects of all the singlet dependent terms on the upper 2×2 block of the mass matrices (CP-odd, CP-even, and charged) purely by redefinitions of $B \rightarrow B'$ and $\mu \rightarrow \mu'$ in terms of the VEV of the singlet $\langle N \rangle = x$ and by including the effects of the λ dependent quartic term.

We further note that we could obtain identical results with an arbitrary number of singlets, since we can always rotate so that only one of them couples to $H_1 H_2$ and the remainder simply complicate the form of f and of the soft terms, which we are essentially regarding as arbitrary. With one singlet, the most general superpotential is

$$W = -\mu H_1 H_2 + \lambda N H_1 H_2 - \frac{k}{3} N^3 + \frac{1}{2} \mu' N^2 + \mu'' N \quad (3.3)$$

In the limit that $\mu, \mu' \mu'' \rightarrow 0$, the above superpotential reduces to that of the NMSSM[3], while if N is removed it reduces to that of the MSSM.

The mass matrix for the CP-odd scalars in the basis (H_1, H_2, N) is a complicated 3-dimensional generalisation of M_A^2 in the MSSM. With only minimal risk of ambiguity

we shall use the same notation for such generalisations as for the MSSM. The tree-level CP-odd mass squared matrix becomes :

$$M_A^2 = \begin{pmatrix} m_{12}'^2 t_\beta & m_{12}'^2 & \cdot \\ m_{12}'^2 & m_{12}'^2 / t_\beta & \cdot \\ \cdot & \cdot & \cdot \end{pmatrix} \quad (3.4)$$

where $m_{12}'^2 = -B'\mu'$. The CP-odd matrix has its Goldstone modes isolated by

$$UM_A^2U^\dagger \equiv \begin{pmatrix} 0 & 0 & 0 \\ 0 & m_A'^2 & \cdot \\ 0 & \cdot & \cdot \end{pmatrix} \quad (3.5)$$

where U is given by

$$U = \begin{pmatrix} c_\beta & -s_\beta & 0 \\ s_\beta & c_\beta & 0 \\ 0 & 0 & 1 \end{pmatrix} \quad (3.6)$$

Clearly m_A' is the analogue of m_A of the MSSM, and $m_A'^2 = m_{12}'^2 / (s_\beta c_\beta)$. The entries in these matrices represented by dots are complicated functions of soft terms and parameters from f and the extended soft potential, and since f is arbitrary they are essentially unconstrained. We define the matrix V_A which diagonalises M_A^2 as follows

$$(V_A U) M_A^2 (V_A U)^\dagger = \text{diag}(0, m_{A_1}^2, m_{A_2}^2) \quad (3.7)$$

where we have taken $m_{A_1} < m_{A_2}$ and V_A can be represented in terms of one mixing angle γ

$$V_A = \begin{pmatrix} 1 & 0 & 0 \\ 0 & c_\gamma & s_\gamma \\ 0 & -s_\gamma & c_\gamma \end{pmatrix} \quad (3.8)$$

As regards the charged Higgs sector, the singlets obviously cannot mix with charged scalars, and we find that (at tree-level) the mass of the charged Higgs is given by

$$m_{H^\pm}^2 = m_A'^2 + M_W^2 - \lambda^2 \nu^2 \quad (3.9)$$

We can immediately obtain the MSSM results by simply setting $\lambda = 0$ and removing all of the singlet terms from the mass matrices. Clearly a non-zero λ tends to reduce the charged scalar masses which can be arbitrarily small.

The CP-even mass squared matrix is now a 3×3 matrix in the basis (H_1, H_2, N) which may be written as

$$M^2 = \begin{pmatrix} M_Z^2 c_\beta^2 + m_A'^2 s_\beta^2 & -(M_Z^2 + m_A'^2 - 2\lambda^2 \nu^2) s_\beta c_\beta & \cdot \\ -(M_Z^2 + m_A'^2 - 2\lambda^2 \nu^2) s_\beta c_\beta & M_Z^2 s_\beta^2 + m_A'^2 c_\beta^2 & \cdot \\ \cdot & \cdot & \cdot \end{pmatrix} \quad (3.10)$$

where, as before, the dots indicate complicated entries. As in the MSSM the CP-even Higgs matrix is diagonalised by

$$VM^2V^\dagger = \text{diag}(m_{h_1}^2, m_{h_2}^2, m_{h_3}^2) \quad (3.11)$$

where V is some complicated 3×3 matrix. Note that we have now chosen to order the mass eigenstates as

$$m_{h_1} < m_{h_2} < m_{h_3} \quad (3.12)$$

so that the definition of V here does *not* reduce to that of V defined earlier where the eigenvalues are conventionally ordered oppositely. For example in the MSSM if we had required that the CP-even Higgs matrix were diagonalised as $VM^2V^\dagger = \text{diag}(m_h^2, m_H^2)$ then V would have to include a re-ordering of the mass eigenstates, and would have been given by

$$V = \begin{pmatrix} -s_\alpha & c_\alpha \\ -c_\alpha & -s_\alpha \end{pmatrix} \quad (3.13)$$

where α is the angle defined earlier in the MSSM. It is to this form that our generalised V must reduce in the MSSM limit.

As in the MSSM we observe that if we do not diagonalise M^2 but instead rotate to a basis where the second Higgs doublet does not have any VEV, then the 11 element of the matrix gives a useful upper bound on the lightest CP-even Higgs mass [5]. This rotation is given by $WM^2W^\dagger = M'^2$ where

$$W = \begin{pmatrix} c_\beta & s_\beta & 0 \\ -s_\beta & c_\beta & 0 \\ 0 & 0 & 1 \end{pmatrix} \quad (3.14)$$

and the bound is given by

$$m_{h_1}^2 \leq M_{11}'^2 = M_Z^2 \cos^2 2\beta + \lambda^2 \nu^2 \sin^2 2\beta \quad (3.15)$$

The reason why this bound is useful is simply that it has no $m_A'^2$ dependence. For example a less useful bound is,

$$m_{h_1}^2 \leq M_{22}'^2 = (M_Z^2 - \lambda^2 \nu^2) \sin^2 2\beta + m_A'^2 \quad (3.16)$$

Starting from the primed basis the CP-even Higgs matrix is diagonalised by

$$X M'^2 X^\dagger = \text{diag}(m_{h_1}^2, m_{h_2}^2, m_{h_3}^2) \quad (3.17)$$

where $X = VW^\dagger$.

We shall define the relative couplings $R_i \equiv R_{ZZh_i}$ as the ZZh_i coupling in units of the standard model ZZh coupling, and similarly we shall define a $Zh_i A_j$ coupling factor $R_{Zh_i A_j}$. For example R_{ZZh_1} is a generalisation of $\sin(\beta - \alpha)$ and the $R_{Zh_1 A_i}$ are generalisations of $\cos(\beta - \alpha)$ in the MSSM. In our notation we find, using the results of Ellis *et al* [3],

$$\begin{aligned} R_i &= \cos \beta V_{i1} + \sin \beta V_{i2} \\ &= (VW^\dagger)_{i1} = X_{i1}. \end{aligned} \quad (3.18)$$

The $Zh_i A_j$ coupling factorises into a CP-even factor S_i and a CP-odd factor P_j [3]

$$R_{Zh_i A_j} = S_i P_j \quad (3.19)$$

where

$$\begin{aligned} S_i &= -V_{i1} \sin \beta + V_{i2} \cos \beta \\ &= (WV^\dagger)_{2i} = X_{i2} \end{aligned} \quad (3.20)$$

and

$$P_j = (V_A U)_{(j+1)2} \cos \beta + (V_A U)_{(j+1)1} \sin \beta \quad (3.21)$$

Eq.(3.21) implies the simple intuitive results

$$P_1 = \cos \gamma, \quad P_2 = -\sin \gamma \quad (3.22)$$

where γ defined in Eq.(3.8) is the angle which controls the amount of singlet mixing in the CP-odd sector.

4 Implementing the Bound on h_1

In this section we shall consider the absolute upper bound on the mass of the lightest CP-even state in this model, using Eq.(3.15) plus radiative corrections. For notational ease we shall first define

$$\Lambda^2 \equiv M_{11}^{\prime 2}. \quad (4.1)$$

Thus the bound is simply

$$m_{h_1}^2 \leq \Lambda^2 \quad (4.2)$$

Clearly Λ^2 is a function of $\tan \beta$ and λ , $\Lambda^2(\tan \beta, \lambda)$, and to find the absolute upper bound we must maximise this function so that

$$m_{h_1}^2 \leq \Lambda_{max}^2 \quad (4.3)$$

where Λ_{max}^2 is the maximum value of $\Lambda^2(\tan \beta \text{ and } \lambda)$,

$$\Lambda_{max}^2 \equiv \max(\Lambda^2(\tan \beta, \lambda)). \quad (4.4)$$

Our task in this section is therefore to find Λ_{max}^2 in the presence of radiative corrections.

It is well known that radiative corrections, which we have so far ignored, drastically affect the bound [6]. In order to deal with these radiative corrections many techniques have been proposed [2]. Here we shall follow the method proposed in ref.[8], which we shall briefly review. According to this method a scale M_{susy} is defined by $M_{susy}^2 = (m_{\tilde{t}_1}^2 + m_{\tilde{t}_2}^2)/2$ where $m_{\tilde{t}_i}$ are the stop mass eigenvalues, and the couplings h_t and h_b found at this scale. Here the squarks are integrated out, leaving an effective Higgs potential involving Yukawa couplings with boundary conditions which differ from the tree-level ones by some finite corrections [2]. Then the Yukawa couplings (including h_t) are run from M_{susy} down to m_t . Below m_t the Yukawa couplings are approximately constant, and so the Higgs potential may be minimised at this scale. The effects of

the RG running have been estimated analytically, leading to fully analytic results for the Higgs masses which agree well with more elaborate methods [8].

For $\lambda = 0$ (as in the MSSM) the bound is obviously largest for $\cos^2(2\beta) = 1$. Given the restricted range $\pi/4 \leq \beta \leq \pi/2$ this implies that the bound is maximised for $\beta = \pi/2$, $\cos 2\beta = -1$, corresponding to $\tan \beta = \infty$ (or in practice its maximum allowed value). However, for sufficiently large λ the tree-level bound will be maximised for $\tan \beta$ equal to its minimum value. In order to obtain an absolute upper bound, we must thus derive an upper limit on λ , which will turn out to be a function of $\tan \beta$. This can be done by demanding that all of the Yukawa couplings remain perturbative up to the GUT scale [5, 6, 4].

We have used the newly discovered mass of the top quark [9] and the two loop SUSY RG equations in the NMSSM [10] to derive an upper bound on λ (defined at m_t , and calculated by requiring all Yukawa couplings h_t , h_b and λ to remain perturbative up to a scale of 10^{16}GeV), which we show as a function of $\tan \beta$ in Figure 1. Results are shown for various values of m_t and $\alpha_3(M_Z)$, and it is likely that the errors from these two measurements will greatly dominate any other uncertainties of our calculation. The main features of this graph are that λ has an upper bound of around 0.5 to 0.7 for intermediate $\tan \beta$, while for large (small) $\tan \beta$ the triviality constraints on h_b (h_t) force this upper bound very rapidly to zero.

In Figure 1, we have assumed that the effect of any other Yukawa couplings in the singlet sector of the superpotential is negligible, but in fact such couplings can have a significant impact, as shown in Figure 2, where we fix $\tan \beta$ and explore the dependence of the upper bound on λ as a function of the coupling k defined in Eq. (3.3) for a model with only one singlet. The most important feature of this figure is that it clearly displays how adding extra Yukawa couplings will always *reduce* the bound on λ , since these will always appear with the same sign in the RG equations.

The reason why λ falls so rapidly to zero above a certain value of k is that here k is approaching its triviality limit, while for small k its impact on the upper bound of λ is negligible.

In Figures 3a to 3c, we plot the bound Λ as a function of $\tan\beta$, M_{susy} , and m_t respectively. For each of these figures, we set the squark soft masses squared m_Q^2 , m_T^2 , and m_B^2 to be equal, and we allow the trilinear squark–Higgs coupling A_t , λ and, except in Figure 3a, $\tan\beta$ to take on the values which maximise the bound. In Figures 3a,3c we select M_{susy} as defined previously to be 1TeV, and in Figures 3a and 3b we select $m_t=175\text{GeV}$. We display bounds for both the MSSM (lower dashed line) and its extension with a singlet. Note that for extreme values of $\tan\beta$ the maximum allowed value of λ falls rapidly to zero, and so the two bounds are then the same, while the same happens for very large m_t since here h_t is again close to triviality. Thus the large value of m_t preferred by *CDF* [9] means that the two bounds are now within around 8GeV. However, it is important to realise that one of the main problems for LEP2 will be that for the MSSM small $\tan\beta$ always gives a light CP-even Higgs, while this need no longer be true in a non-minimal extension, thus seriously damaging the prospects for particle searches.

5 LEP2 Search Strategies

5.1 $Z \rightarrow Zh_i$ and General Bounds on CP-even Higgses

Recently upper bounds on all three neutral CP-even Higgs scalars in the general extension of the MSSM with a single gauge singlet superfield have been derived [7]. The basic observation which follows from Eq.(3.17) and the definition $M_{11}^2 \equiv \Lambda^2$ is: ¹

$$\begin{aligned}\Lambda^2 &= X_{11}^2 m_{h_1}^2 + X_{21}^2 m_{h_2}^2 + X_{31}^2 m_{h_3}^2 \\ &= R_1^2 m_{h_1}^2 + R_2^2 m_{h_2}^2 + R_3^2 m_{h_3}^2\end{aligned}\tag{5.1}$$

¹Note that X is real if the Higgs sector conserves CP.

where we have used the fact that $R_i = X_{i1}$. Eq.(5.1) together with Eq.(3.12) clearly implies

$$\Lambda^2 \geq (R_1^2 + R_2^2 + R_3^2)m_{h_1}^2 \quad (5.2)$$

and given that

$$R_1^2 + R_2^2 + R_3^2 = 1 \quad (5.3)$$

by the unitarity of X , we find the usual bound in Eq.(3.15),

$$m_{h_1}^2 \leq \Lambda^2 \quad (5.4)$$

Using a similar argument, a bound on the h_2 mass may be obtained from Eq.(5.1) :

$$m_{h_2}^2 \leq \frac{\Lambda^2 - R_1^2 m_{h_1}^2}{1 - R_1^2} \quad (5.5)$$

$m_{h_3}^2$ is given from Eq.(5.1) by

$$m_{h_3}^2 = \frac{\Lambda^2 - R_1^2 m_{h_1}^2 - R_2^2 m_{h_2}^2}{1 - R_1^2 - R_2^2} \quad (5.6)$$

from which we can extract a bound

$$m_{h_3}^2 \leq \frac{\Lambda^2 - (R_1^2 + R_2^2)m_{h_1}^2}{1 - R_1^2 - R_2^2} \quad (5.7)$$

As we shall see, Eqs.(5.5) and (5.7) are useful upper bounds on m_{h_2} and m_{h_3} in terms of $m_{h_1}^2$, R_1 , R_2 and $\Lambda^2 \equiv M_{11}'^2$ (which is just the bound on $m_{h_1}^2$). These bounds tightly constrain the spectrum in terms of the couplings and hence will allow us to study the reach of colliders when the mixing parameters take on arbitrary values.

The above general bounds are useful since h_1 may be light but very weakly coupled. In the MSSM this can happen when $\sin(\beta - \alpha)$ becomes small. In the present model R_1 can also be small because h_1 may contain a large singlet component. In this case it does not matter how light h_1 is since its couplings may be so weak that it can never be detected. At first sight this seems to be a catastrophe for LEP2 where in the MSSM h_1 is usually the easiest state to find. However, if $R_1 \approx 0$ we may simply

ignore h_1 and concentrate on h_2 which then becomes the lightest physically coupled CP-even state. Moreover it can be seen from Eq.(5.5) that if $R_1 \rightarrow 0$ then h_2 must satisfy

$$m_{h_2}^2 \leq \Lambda^2 \quad (5.8)$$

which is just the bound on m_{h_1} . In other words, if the lightest CP-even state is essentially invisible, then the second lightest CP-even state must be quite light, and may be within the reach of LEP2. Similarly if both R_1 and R_2 are ≈ 0 then Eq.(5.6) implies that

$$m_{h_3}^2 = \Lambda^2 \quad (5.9)$$

The above restrictions on the Higgs masses and couplings imply that a collider of a given energy and integrated luminosity will be able to exclude values of Λ below which it is impossible for all the Higgses to have simultaneously escaped detection.

We shall discuss this further in Section 5.3.

5.2 Exclusion Plots in the $R^2 - m_h$ Plane at LEP

In this sub-section we shall be concerned with exclusion plots in the $R^2 - m_h$ plane such as those that have already been obtained at LEP1 and whose possible form at LEP2 has been predicted, where $R^2 \equiv \sin^2(\beta - \alpha)$ in the MSSM. LEP1 has not discovered a CP-even Higgs boson [11], and this non-observation has enabled a 95% CL exclusion limit to be extracted on the value of the square of the relative ZZh coupling R^2 , as a function of the CP-even Higgs mass m_h extending out to $m_h = 65$ GeV[12]. Similar exclusion plots at LEP2 will extend the Higgs mass range to $m_h > 65$ GeV leading to possible exclusion curves whose precise shape will depend on the energy and integrated luminosity of LEP2[13]. Three different sets of LEP2 machine parameters have been considered corresponding to energies and integrated

luminosities per experiment of [13]

$$\begin{aligned}
\sqrt{s} &= 175 \text{ GeV}, \quad \int \mathcal{L} = 150 \text{ pb}^{-1} \\
\sqrt{s} &= 192 \text{ GeV}, \quad \int \mathcal{L} = 150 \text{ pb}^{-1} \\
\sqrt{s} &= 205 \text{ GeV}, \quad \int \mathcal{L} = 300 \text{ pb}^{-1}.
\end{aligned} \tag{5.10}$$

The existing LEP1 [12] and anticipated LEP2 [13] exclusion plots are combined in Fig.4a, for the three different LEP2 scenarios, and assuming a 100% h_1 branching fraction into $\bar{b}b$. The very steep rise of the contours means that, if a standard model-like Higgs boson of a certain fixed mass can be produced at LEP (corresponding to $R^2 = 1$) then reducing R_{ZZh}^2 has little effect on its visibility until R_{ZZh}^2 becomes quite small. The relatively flat LEP1 regions of the contours correspond to minimum threshold values of R_{ZZh}^2 below which nothing can be seen for any value of the mass.

The above exclusion plots in Fig.4a are the result of a sophisticated Monte Carlo simulation of the LEP detectors. It is interesting to observe that these contours roughly correspond to the value of the coupling R^2 which would yield 50 Higgs events of a given mass. The plot of contours of 50 h events as a function of m_h and R^2 for the three different LEP2 machine scenarios is shown for comparison in Fig.4b. Note that this simple parameterisation of the exclusion plots of Fig.4a fails badly for $m_h \approx M_Z$, and also the actual exclusion limits from LEP1 are significantly stronger than our LEP2 approximation for small Higgs masses. Nevertheless Fig.4b provides a useful caricature of the exclusion plots in Fig.4a.

Finally note that the exclusion plots in Fig.4 may be interpreted for each of the three CP-even Higgs bosons in this model taken separately. In other words the disallowed region to the upper and left of the lines will exclude values of R_1^2 for a given m_{h_1} , and similarly for the other two CP-even Higgs bosons.

5.3 Excluded Values of Λ

Although there are a large number of parameters in this model, and three CP-even Higgs bosons, it proves possible to exclude values of Λ smaller than a certain amount, where Λ is defined as above to be the upper bound on the lightest CP-even Higgs boson, and is to be regarded as a function of $\lambda, \tan\beta$ and all the other parameters which enter the calculation of radiative corrections such as the top mass, the squark masses, and so on. If LEP2 does not discover any CP-even Higgs bosons then exclusion plots such as those in Fig.4a may be produced. We now show that such exclusion plots may be used to place an excluded lower limit on the value of Λ in this model. If the excluded lower limit on Λ reaches the theoretical upper limit of about 146 GeV (dependent on the top mass and SUSY spectrum as discussed above) then the model is excluded. For example, a linear collider of energy 300 GeV should be able to exclude the model [7]. We now describe how LEP may be used to exclude values of Λ in this model.

Clearly a specified value of Λ is consistent with many sets of values of the parameters m_{h_i}, R_i subject to the bounds discussed in section 5.1. In general some of these sets of m_{h_i}, R_i will lead to one or more CP-even Higgs boson in the excluded (upper left) part of Fig.4a and some sets will lead to Higgs bosons only in the allowed region. This means that, for a given Λ , one or more CP-even Higgs bosons may or may not be discovered at LEP2, depending on the values of the other (complicated unknown) parameters in the model. According to our discussion in Section 5.1, it is clear that as Λ is reduced, more and more of the allowed sets of m_{h_i}, R_i will move into the excluded part of Fig.4a. As Λ is reduced below some critical value all the sets of values of m_{h_i}, R_i will eventually fall into the excluded region of Fig.4a. This critical value of Λ is the maximum value of Λ excluded by LEP. This implies that the maximum excluded value of Λ is determined by whether the “worst case” (*i.e.*

hardest to see experimentally) values of m_{h_i}, R_i consistent with this value of Λ lie within the allowed region or not.

In order to determine the “worst case” parameters we first fix Λ at some specified value (less than its maximum as determined in section 4) and then we scan over values of m_{h_1} from zero up to Λ . For each value of m_{h_1} we set R_1 equal to the maximum allowed value as shown in Fig.4a (or 1 if this would require $R_1 > 1$). For Λ, m_{h_1} and R_1 fixed as above, we then scan over m_{h_2} from m_{h_1} up to its upper bound which is now fixed according to Eq.(5.5). For each value of m_{h_2} we set R_2 equal to its maximum allowed value as before. For $\Lambda, m_{h_1}, m_{h_2}, R_1$ and R_2 fixed as above, m_{h_3} and R_3 are now completely specified by Eqs.(5.3) and (5.6). If R_3 is larger than its maximum allowed value (according to Fig.4b), then the “worst case” with the given values of m_{h_1} and m_{h_2} is excluded. If all the “worst case” points in the m_{h_1}, m_{h_2} scan turn out to be excluded then we conclude that this value of Λ is excluded by LEP.

According to Eq.(3.15), the value of $\Lambda^2 \equiv M_{11}'^2$ is a function of λ and $\tan\beta$, plus parameters which enter in the radiative corrections. For a given value of λ , and given radiative correction parameters, the exclusion limit on Λ may be interpreted as an exclusion limit on $\tan\beta$ in this model, independently of m_A' . Thus the present analysis will yield a horizontal exclusion line in the $m_A' - \tan\beta$ plane, as we shall see in Section 6.

If the observability criterion above is replaced by the approximate exclusion limit obtained from 50 higgs events regardless of branching fractions, as in Fig.4b, then the above algorithm can be solved analytically. In this simple case, the “worst case” for LEP2 to discover would be one where the largest of the three cross-sections σ_i was minimised, where

$$\sigma_i = \sigma(e^+e^- \rightarrow Zh_i) = \sigma_{SM}(e^+e^- \rightarrow Zh)|_{m_h=m_{h_i}} R_i^2 \quad (5.11)$$

It is not hard to show that this will occur when $\sigma_1 = \sigma_2 = \sigma_3$, and hence when

$\sum_i \sigma_{SM}(m_{h_i}) R_i^2$ is minimised. Using the constraints in Eqs.(5.1) and (5.3), together with the analytical form for the mass dependence of the tree-level cross-section,

$$\sigma_{SM}(m_{h_i}) \sim \lambda^{1/2}(\lambda + 12sm_Z^2) \quad (5.12)$$

where $\lambda = (s + (M_Z + m_h)^2)(s - (M_Z - m_h)^2)$, it is then straightforward to prove that this will always be minimised when all three masses are degenerate and $R_i^2 = 1/3$.

This simple result leads to the contour plot of $\Lambda = \sqrt{M_{11}^2}$ in the integrated luminosity-energy plane shown in Fig.5. ² Along each of the contours the energy and integrated luminosity correspond to at least one CP-even Higgs boson being produced with a yield of 50 events, for any allowed choice of m_{h_1} and m_{h_2} . Thus this contour plot is an estimate of the values of Λ which may be excluded for different machine parameters. For example, LEP2 with an energy of 205 GeV will place a limit $\Lambda > 100$ GeV, depending on the integrated luminosity. For this energy there is a rapid increase in the reach of Λ from 10-100 GeV as the luminosity is increased from 100-400 pb⁻¹, followed by a very slow increase if the luminosity is increased beyond this.

To summarise, the worst case parameters are when all the three CP-even Higgs bosons have a mass equal to $m_{h_i} = \Lambda$ and equally suppressed couplings $R_i^2 = 1/3$. In fact since in this case there are three Higgs bosons to discover the cross-section will be three times larger than for each Higgs boson taken separately. Nevertheless, it is clear that for sets of parameters when the Higgs boson masses are not degenerate and the Higgs bosons must be considered separately the worst case will never be worse than that just described. The excluded value of Λ is therefore simply determined by the following rule of thumb: consider a single Higgs boson with a coupling equal to $R^2 = 1/3$, and find its maximum excluded mass for a given set of machine parameters, then equate this mass with the maximum excluded value of Λ .

²Note that this is *total* luminosity, not luminosity per experiment as elsewhere in this paper.

According to this rule of thumb, LEP1 already places a limit on Λ of $\Lambda > 59$ GeV, which is just equal to the mass limit for a CP-even Higgs boson with its ZZh coupling suppressed by $R^2 = 1/3$. Note that because of the steep rises of the function plotted in Fig.4a, the excluded values of Λ are not far from the present excluded value of SM Higgs boson mass of about 65 GeV. Similarly we find that LEP2 will yield the exclusion limits $\Lambda > \Lambda_{min} = 81, 93, 105$ GeV, for the three sets of LEP2 machine parameters in Eq.(5.10), respectively.

The above rule of thumb is easily extended to the more general case of n singlets being added to the MSSM, *i.e.* the (M+n)SSM. In such a model the worst case will correspond to $2 + n$ CP-even Higgs bosons each having a mass equal to Λ , and each having a coupling suppression relative to the SM of $R^2 = 1/(2 + n)$. The excluded value of Λ is determined from the exclusion plot of a Higgs boson with a coupling equal to $R^2 = 1/(2 + n)$. For example for $n = 1, 2, 3$ we find that $R^2 = 1/3, 1/4, 1/5$ corresponding to the LEP1 excluded values given from Fig.4a of about $\Lambda > 59, 58, 57.5$ GeV, respectively. We find it remarkable that such strong limits on Λ can be placed on models with several singlets.

We emphasise that this argument is only approximate, and may become unreliable when more realistic Higgs exclusion data as in Fig.4a are used, rather than the simple analytic calculations of how large R_i^2 may become as a function of $m_{h_i}^2$ (as in Fig4b).

Finally note that if Higgs bosons are discovered then this does not mean, in the context of this model, that Λ is small. One may have a large Λ (as large as 146 GeV) and still be lucky enough to find that there is a visible CP-even Higgs boson corresponding to some fortunate values of parameters. All we have shown is how the non-observation of Higgs bosons enables a firm lower limit to be placed on Λ , corresponding to a “worst case” situation. In general, for a given Λ , the true situation will be easier than this, leading to the possibility of Higgs discovery at LEP2 even for

very large Λ .

5.4 $Z \rightarrow hA$

In section 3 it was seen that the $Zh_i A_j$ couplings factorise into a factor from the CP-odd matrix multiplied by a factor from the CP-even matrix [3] given by

$$\begin{aligned} R_{Zh_i A_1} &= S_i \cos \gamma \\ R_{Zh_i A_2} &= -S_i \sin \gamma. \end{aligned} \quad (5.13)$$

Using equation (3.17) we find

$$\begin{aligned} M_{22}'^2 &= X_{12}^2 m_{h_1}^2 + X_{22}^2 m_{h_2}^2 + X_{32}^2 m_{h_3}^2 \\ &= S_1^2 m_{h_1}^2 + S_2^2 m_{h_2}^2 + S_3^2 m_{h_3}^2 \end{aligned} \quad (5.14)$$

where we have used the fact that $S_i = X_{i2}$. Again

$$S_1^2 + S_2^2 + S_3^2 = 1 \quad (5.15)$$

from the unitarity of X . $M_{22}'^2$ just corresponds to the less useful bound in Eq.(3.16). Eq.(5.14) is of course virtually identical to Eq.(5.1), and hence we may immediately write down analogous bounds which relate the masses of the lightest CP-even states to their ZhA couplings :

$$\begin{aligned} m_{h_1}^2 &\leq M_{22}'^2 \\ m_{h_2}^2 &\leq \frac{M_{22}'^2 - S_1^2 m_{h_1}^2}{1 - S_1^2} \\ m_{h_3}^2 &\leq \frac{M_{22}'^2 - (S_1^2 + S_2^2) m_{h_1}^2}{1 - S_1^2 - S_2^2} \end{aligned} \quad (5.16)$$

It is trivial to prove that

$$m_A'^2 = m_{A_1}^2 \cos^2 \gamma + m_{A_2}^2 \sin^2 \gamma \quad (5.17)$$

which is similar to Eqs.(5.1) and (5.14). Eq.(5.17) implies the bound

$$m_{A_1}^2 \leq m_A'^2 \quad (5.18)$$

so that $m'_A{}^2$ is just the upper bound on the lightest CP-odd Higgs boson in this model. When A_1 is weakly coupled ($\cos \gamma \approx 0$), Eq.(5.17) implies that $m_{A_2}{}^2 \approx m'_A{}^2$. Thus if the lighter CP-odd state is weakly coupled, corresponding to its having a large singlet component, then the heavier CP-odd state (which essentially corresponds to the MSSM CP-odd state) sits at the bound, in complete analogy with Eq.(5.6).

We now discuss how LEP limits on the non-observation of $Z \rightarrow hA$ may be used to exclude values of $m'_A{}^2$ and $M'_{22}{}^2$ smaller than a certain amount. The following discussion obviously parallels that of Section 5.3. As before, the “worst case” for $Z \rightarrow hA$ production will provide the best exclusion limit on $m'_A{}^2$ and $M'_{22}{}^2$. In order to determine this worst case we simply repeat the algorithm in Section 5.3, but with the R_i couplings replaced by the S_i couplings in Eq.(5.16). However in the present case we need to generalise this procedure to include the CP-odd parameters m_{A_1} and γ . Using the exclusion criterion of requiring 50 hA events for exclusion, it is readily seen that such a procedure enables the maximum excluded values of $m'_A{}^2$ and $M'_{22}{}^2$ to be obtained.

Similarly to the case of Section 5.3, we find the worst case to correspond to the CP-odd parameters $m_{A_1} = m_{A_2} = m'_A$ and $\gamma = \pi/4$, and the CP-even parameters $S_1 = S_2 = S_3 = 1/\sqrt{3}$ and $m_{h_1} = m_{h_2} = m_{h_3} = M'_{22}$. This corresponds to $R_{Zh_i A_j}{}^2 = 1/6$ in each case. The excluded values of $m'_A{}^2$ and $M'_{22}{}^2$ may be found by using the approximation of 50 hA events with h having a mass equal to M'_{22} , A having a mass equal to m'_A , and the coupling $R_{ZhA}{}^2 = 1/6$, similarly to the $Z \rightarrow Zh$ case discussed above.

As before, the above rule of thumb is easily extended to the more general case of n singlets being added to the MSSM, *i.e.* the $(M+n)$ SSM. In such a model the worst case of hA production will correspond to $n + 2$ CP-even Higgs bosons each having a mass equal to $\sqrt{M'_{22}}$, and each having a coupling factor of $S^2 = 1/(2 + n)$,

plus $n + 1$ CP-odd Higgs bosons each having a mass equal to m'_A , and each having a coupling factor of $P^2 = 1/(1 + n)$. As before, when the states are non-degenerate, there must be at least one pair h_i and A_j which have a cross-section larger than this. For example for $n = 1, 2, 3$, the couplings are $R_{ZhA}^2 = 1/6, 1/12, 1/20$.

We expect this simple approximation to be rather more robust for the $Z \rightarrow hA$ process than for $Z \rightarrow Zh$, because of the more rapid fall-off of the cross-section with increasing masses for the hA process than for Zh . Furthermore, the larger number of parameters here make a more elaborate analysis, such as we shall later perform for $Z \rightarrow Zh$, more difficult. Thus we shall always use this approximate method when we present our results for $Z \rightarrow hA$.

We note that of course $m'_A{}^2$ and $M_{22}'^2$ are not independent parameters. Using Eq.(3.16) the value of $M_{22}'^2$ may be related to $m'_A{}^2$ and, for a given λ and $\tan \beta$, $M_{22}'^2$ may be eliminated. Thus, for a fixed value of λ , we shall present exclusion plots in the $m'_A - \tan \beta$ plane from the non-observation of $Z \rightarrow hA$.

5.5 Charged Higgs Detection

As discussed above, the $Z \rightarrow hA$ and $Z \rightarrow Zh$ searches are less powerful in extended models because the cross-section can be greatly reduced. We now turn to the last feasible search at LEP2, that for charged Higgs production. One feature of the model which was discussed earlier was that the charged Higgs can be lighter than in the MSSM when singlets are included; furthermore, its couplings cannot be suppressed by singlet mixing. Hence the charged Higgs signal, which in the MSSM is completely dominated by $Z \rightarrow hA$, is now far more important.

Charged Higgs discovery is complicated, since the rate is strongly dependent not only on the Higgs mass, which must not be too close to the W or Z mass to allow elimination of background, but also on its branching fractions to cs and $\tau\nu$ which are

determined by $\tan\beta$ [14]. In addition, any LEP2 discovery region may be dominated by study of top quark decays at the TeVatron [15]. For the purposes of this paper we shall adopt the rather optimistic view that LEP2 will have sufficient luminosity so that the kinematic limit may be approached.

6 Exclusion Limits in the m'_A - $\tan\beta$ Plane

In this section we shall present our results as excluded regions in the $m'_A - \tan\beta$ plane, which is familiar from similar studies in the MSSM, and should simplify the comparison of the (M+1)SSM with the MSSM. Let us first briefly summarise the LEP2 search strategies we have so far introduced in Section 5.

For the process $Z \rightarrow h_i A_j$ (discussed in section 5.4) we have shown how LEP2 can be used to place exclusion limits on m'_A ² and M_{22}^2 . For a fixed value of λ (and radiative correction parameters) these limits may be interpreted as excluded regions in the $m'_A - \tan\beta$ plane. We show both the worst case mixing scenario and the simple scenario where there is no singlet mixing. These are calculated using the simple approximation that 50 $Z \rightarrow hA$ events will be sufficient to ensure a discovery.

Similarly, for the processes $Z \rightarrow Zh_i$ (discussed in sections 5.1-5.3) we have shown how LEP2 can be used to place an exclusion limit on the value of Λ . For a fixed value of λ (and radiative correction parameters) this can be interpreted as an exclusion limit on $\tan\beta$, independently of m'_A (*i.e.* a horizontal exclusion line in the m'_A - $\tan\beta$ plane.) However, as we shall see, the resulting excluded region is not very large, so we shall resort to a more powerful technique as discussed below.

This new technique exploits the fact that the upper 2×2 block of the CP-even mass squared matrix in Eq.(3.10) is completely specified (for fixed λ) in the m'_A - $\tan\beta$ plane. However, unlike the MSSM, the CP-even spectrum is not completely specified since it depends on three remaining unknown real parameters associated with singlet

mixing (*i.e.* the dots in Eq.(3.10).) Each choice of these unconstrained terms then completely specifies the parameters m_{h_i}, R_i , and we can test to see if the resulting Higgs spectrum is excluded or allowed. We then scan over all possible choices (which we parametrise as m_{h_1}, R_1 and one other mixing angle) and if the resulting spectrum can always be excluded by LEP2, then we conclude that this point in the m'_A - $\tan\beta$ plane (for fixed λ) can be excluded.

Since we have presented two separate algorithms for generating $Z \rightarrow Zh_i$ contours, it is worthwhile here mentioning some of the advantages and disadvantages of the different techniques. The method of scanning over the whole of parameter space is naturally better than the algorithm based on the exclusion limit of Λ , in the sense that it gives a better reach in the plane. This is clear from the fact that we are considering a general 3×3 mass matrix which has the upper 2×2 block given by our position in the $m'_A - \tan\beta$ plane, while the bound algorithm in section 5.3 allows any mass matrix which has the correct 11 component in a particular basis (which is why the exclusion contours derived in this way do not have any m_A dependence). On the other hand, the scanning technique is very CPU-intensive, and would rapidly become even more so if we allowed extra singlet states. In addition, it is hard to understand these results analytically, whereas the simple arguments in section 5.3 based around Eq.(5.1) are much more straightforward. Hence both techniques are worth considering.

6.1 $\lambda = 0$

In figures 6-8 we consider the impact of mixing only, with λ set equal to zero. This may not be as unreasonably optimistic as it sounds, since recent GUT scale analyses [16, 10] have concluded that very small λ is preferred with universal soft parameters. In each case we show the charged Higgs kinematic limit as a dot-dashed line. The two $Z \rightarrow hA$ exclusion contours are represented by dashed lines and drawn with the

assumption of worst case mixing (left) and of no singlet mixing (right). The three $Z \rightarrow Zh$ exclusion contours are represented by solid lines, and shown for the case of no singlet mixing (uppermost line), the full scan over parameter space (middle line), and for the bound algorithm (lower horizontal line) discussed in detail in section 5.3. The no singlet mixing lines with $\lambda = 0$ simply correspond to the MSSM.

Figure 6 shows the exclusion contours for $\sqrt{s} = 175\text{GeV}$, and integrated luminosity of 150pb^{-1} per experiment. Figure 7 is identical but with $\sqrt{s} = 192\text{GeV}$, while Figure 8 has $\sqrt{s} = 205\text{GeV}$ and integrated luminosity of 300pb^{-1} per experiment. All these figures have $m_t = 175\text{GeV}$, degenerate squarks at 1TeV , and $\alpha_3(M_Z) = 0.12$.

In each of these figures it is clear that the charged Higgs kinematic limit discovery line (which, as mentioned above, is rather over-optimistic as a discovery process, but is nevertheless indicative of where this process will become important) is completely superseded by the $Z \rightarrow hA$ line, although to a rather less extreme degree than in the MSSM. The inclusion of singlets reduces the excluded region for both $Z \rightarrow hA$ and $Z \rightarrow Zh$ quite substantially relative to the MSSM, but still leaves reasonably large areas covered. Simply using the bound algorithm however gives rather poorer reach.

6.2 $\lambda > 0$

To show how large λ affects our results, in Figure 9 we show a figure with $\sqrt{s} = 192\text{GeV}$, and integrated luminosity of 150pb^{-1} per experiment, but with $\lambda = 0.5$. Here the charged line is becoming quite competitive with the $Z \rightarrow hA$ line, and so a charged Higgs search may well be the most practical one at LEP2. The $Z \rightarrow hA$ contours are hardly changed from those in the $\lambda = 0$ case except for very small $\tan\beta$.

The most significant impact is however on the $Z \rightarrow Zh$ lines. Here even the no mixing scenario has very little reach in the $m_A - \tan\beta$ plane because, as is clear from Eq.(3.15), small $\tan\beta$ no longer implies a light CP-even state. With singlet mixing,

no part of the plane can be covered at all.

7 Conclusion

The addition of extra singlets to the MSSM greatly complicates the model and renders far harder the main experimental searches. However it is possible to exclude this model by placing an experimental lower bound Λ_{min} on the value of the parameter Λ which is just the upper bound on the lightest CP-even Higgs boson mass. In the limit that the lightest CP-even Higgs boson is very weakly coupled, this bound applies to the second lightest CP-even Higgs boson. Thus for a fixed value of Λ the entire CP-even Higgs boson spectrum is constrained, resulting in experimentally excluded values of Λ associated with the “worst case” scenarios discussed in section 5.3.

We have seen that LEP1 already finds $\Lambda > \Lambda_{min} = 59$ GeV, and LEP2 will set limits of $\Lambda_{min} \approx 81, 93, 105$ GeV for three different levels of operation. The theoretical upper bound on Λ is $\Lambda_{max} \approx 146$ GeV, depending on the details of the squark spectrum and on the top mass. Once Λ_{min} becomes greater than or equal to Λ_{max} then the model will be excluded. We have generalised this procedure to the case of an arbitrary number of extra singlets. Thus our first conclusion is that it will be possible to exclude a version of the MSSM containing additional singlets.

The effects of the additional singlet can be thought of as reducing the Higgs sector of the model to the MSSM with two additional complicating factors : extra singlet states which can mix in an arbitrary way with the usual neutral Higgs states altering the masses and diluting the couplings of the mass eigenstates; and an extra Higgs sector quartic coupling λ which changes the mass matrices even in the absence of singlet mixing.

We have systematically studied the case of singlet mixing with $\lambda = 0$, with the primary conclusion that, while the inclusion of a singlet can significantly complicate

matters for searches at LEP2, it is still possible to cover a significant amount of the $m'_A - \tan \beta$ plane using the usual $Z \rightarrow Zh$ and $Z \rightarrow hA$ searches. The main difference in strategy between the searches in the MSSM and in models with singlets is that more luminosity is needed to cover the same area of the plane, since states can be more weakly coupled than in the MSSM. A second difference is that, because singlets cannot mix with charged states, the charged Higgs signal cannot be degraded and so is more important than in the MSSM where it is completely dominated by $Z \rightarrow hA$.

The effect on non-zero λ is more troublesome. For large λ the mass bounds in the MSSM are markedly increased, particularly at small $\tan \beta$ which is of course the region where LEP2 normally has the best reach. This largely wrecks the prospect of excluding large parts of the $m'_A - \tan \beta$ plane through the process $Z \rightarrow Zh$, and has some impact on $Z \rightarrow hA$. However, we note that large λ also reduces the charged Higgs mass substantially, making its discovery easier.

We conclude on a positive note by pointing out that for much of this paper we have assumed worst case mixing scenarios, and considered how it might be possible to rule out regions of parameter space in a consistent way for arbitrary parameters from the singlet sector. For the MSSM, specifying a point in the $m_A - \tan \beta$ plane completely specifies all the masses and mixings, and so points outside the discovery contours cannot be discovered; however with singlets it is possible that, if we are lucky enough, *any* point in the $m'_A - \tan \beta$ plane could lead to a discovery, since it is possible to construct singlet mixing parameters which will reduce the mass of a heavy CP-even state while leaving its coupling reasonably large. Hence we can argue that despite the rather negative impact of the mixing on the LEP2 exclusion contours, a SUSY Higgs discovery may be no less likely in a model with singlets than in the MSSM.

Acknowledgements

We would like to thank the LEP2 Higgs working group and particularly M. Carena, U. Ellwanger, H. Haber, C. Wagner, and P. Zerwas for many stimulating discussions and for encouraging us finally to do some work on this topic. We are also very grateful to P. Janot and A. Sopczak for sharing their data and expertise.

References

- [1] For reviews see for example H.P. Nilles, *Phys. Rep.* **110** (1984) 1; H.E. Haber and G.L. Kane, *Phys. Rep.* **117** (1985) 75.
- [2] H. Haber and R. Hempfling, *Phys. Rev. Lett.* **66** (1991) 1815;
Y. Okada, M. Yamaguchi and T. Yanagida, *Prog. Theor. Phys.* **85** (1991) 1;
Phys. Lett. **B262** (1991) 54;
J. Ellis, G. Ridolfi and F. Zwirner, *Phys. Lett.* **B257** (1991) 83; *Phys. Lett.* **B262** (1991) 477;
A. Brignole, J. Ellis, G. Ridolfi and F. Zwirner, *Phys. Lett.* **B271** (1991) 123;
A. Brignole, *Phys. Lett.* **B277** (1992) 313; *Phys. Lett.* **B281** (1992) 284;
J.L. Lopez and D.V. Nanopoulos, *Phys. Lett.* **B266** (1991) 397;
K. Sasaki, M. Carena and C.E.M. Wagner, *Nucl. Phys.* **B381** (1992) 66;
H.E. Haber and R. Hempfling, *Phys. Rev.* **D48** (1993) 4280.
- [3] P. Fayet, *Nucl. Phys.* **B90** (1975) 104;
J. Ellis, J.F. Gunion, H.E. Haber, L. Roszkowski and F. Zwirner, *Phys. Rev.* **D39** (1989) 844;
L. Durand and J.L. Lopez, *Phys. Lett.* **B217** (1989) 463;
M. Drees, *Int. J. Mod. Phys.* **A4** (1989) 3635.
- [4] T. Elliott, S.F. King, P.L. White, *Phys. Rev.* **D49** (1994) 2435.

- [5] J.R. Espinosa and M. Quiros, *Phys. Lett.* **B279** (1992) 92;
 G. Kane, C. Kolda and J. Wells, *Phys. Rev. Lett.* **70** (1993) 2686;
 J.R. Espinosa and M. Quiros, *Phys. Lett.* **B302** (1993) 51.
- [6] U. Ellwanger and M. Rausch de Traubenberg, *Z. Phys.* **C53** (1992) 521;
 U. Ellwanger and M. Lindner, *Phys. Lett.* **B301** (1993) 365;
 U. Ellwanger, *Phys. Lett.* **B303** (1993) 271;
 W. ter Veldhuis, Purdue preprint PURD-TH-92-11 and hep-ph/9211281;
 T. Elliott, S.F. King and P.L. White, *Phys. Lett.* **B305** (1993) 71;
 T. Elliott, S.F. King and P.L. White, *Phys. Lett.* **B314** (1993) 56.
- [7] J. Kamoshita, Y. Okada and M. Tanaka, *Phys. Lett.* **B328** (1994) 67.
- [8] M. Carena, J. Espinosa, M. Quiros, C. Wagner, *Phys. Lett.* **B355** (1995) 209.
- [9] The CDF Collaboration, *Phys. Rev. Lett.* **73** (1994) 225; *Phys. Rev.* **D50** (1994) 2966; *Phys. Rev. Lett.* **74** (1995) 2626;
 The D0 Collaboration, *Phys. Rev. Lett.* **74** (1995) 2632.
- [10] T. Elliott, S.F. King, P.L. White, *Phys. Lett.* **B351** (1995) 213;
 S. F. King and P. L. White, *Phys. Rev.* **D52** (1995) 4183.
- [11] The ALEPH collaboration, *Phys. Lett.* **B313** (1993) 299;
 The DELPHI collaboration, *Nucl. Phys.* **B373** (1992) 3; *Nucl. Phys.* **B421** (1994) 3;
 The L3 collaboration, *Phys. Lett.* **B303** (1993) 391;
 The OPAL collaboration, *Phys. Lett.* **B253** (1991) 511; *Phys. Lett.* **B327** (1994) 397.
- [12] A. Sopczak, CERN-PPE-95-046, hep-ph/9504300, and proceedings of the IX International Workshop on High Energy Physics, Moscow, 1994;
 P. Janot, private communication.

- [13] P. Janot, private communication.
- [14] A. Sopczak, *Int. J. Mod. Phys. A* **9** (1994) 1747;
A. Sopczak, *Z. Phys.* **C65** (1995) 449.
- [15] V. Barger, R.J.N. Phillips, *Phys. Rev.* **D41** (1990) 884;
A.C. Bawa, C.S. Kim, A.D. Martin, *Z. Phys.* **C47** (1990) 75;
R.M. Godbole, D.P.Roy, *Phys. Rev.* **D43** (1991) 3640;
M. Drees, D.P. Roy, *Phys. Lett.* **B269** (1991) 155.
- [16] U. Ellwanger, M. Rausch de Traubenberg, C. A. Savoy, *Phys. Lett.* **B315** (1993) 331;
Ph. Brax, U. Ellwanger, C. A. Savoy, *Phys. Lett.* **B347** (1995) 269;
U. Ellwanger, M. Rausch de Traubenberg, C. A. Savoy, *Z. Phys.* **C67** (1995) 665.

8 Figure Captions

Figure 1: Maximum value of $\lambda(m_t)$ as a function of $\tan\beta$, shown for various values of m_t and $\alpha_3(M_Z)$ and derived from requiring perturbativity of all Yukawa couplings up to a scale 10^{16}GeV .

Figure 2: Maximum value of $\lambda(m_t)$ as a function of $k(m_t)$, shown for various values of $\tan\beta$, with $m_t = 175\text{GeV}$ and $\alpha_3(M_Z) = 0.12$ and derived from requiring perturbativity of all Yukawa couplings up to a scale 10^{16}GeV .

Figure 3a: Λ_{max} , the bound on the lightest Higgs in the MSSM with (upper solid line) and without (lower dashed line) added singlets, shown as a function of $\tan\beta$ with $M_{susy} = 1\text{TeV}$, $m_t = 175\text{GeV}$, and λ and A_t set so as to maximise the bound.

Figure 3b: Λ_{max} , the bound on the lightest Higgs in the MSSM with (upper solid line) and without (lower dashed line) added singlets, shown as a function of M_{susy} with $m_t = 175\text{GeV}$, and λ , A_t and $\tan\beta$ set so as to maximise the bound.

Figure 3c: Λ_{max} , the bound on the lightest Higgs in the MSSM with (upper solid line) and without (lower dashed line) added singlets, shown as a function of m_t with $M_{susy} = 175\text{GeV}$, and λ , A_t and $\tan\beta$ set so as to maximise the bound.

Figure 4a: R^2 versus m_h for three different sets of machine parameters at LEP2, using a full analysis of the experimental data. For $m_h \lesssim 50\text{GeV}$ the LEP1 bounds are tighter and so we use those instead. These are 95% confidence level exclusion contours. Points above the line correspond to states which could be seen, those below to those which could not be seen. The three lines are for $\sqrt{s} = 175\text{GeV}$, $\int \mathcal{L} = 150\text{pb}^{-1}$ per experiment; $\sqrt{s} = 192\text{GeV}$, $\int \mathcal{L} = 150\text{pb}^{-1}$ per experiment; $\sqrt{s} = 205\text{GeV}$, $\int \mathcal{L} = 300\text{pb}^{-1}$ per experiment; reading from left to right.

Figure 4b: R^2 versus m_h for three different sets of machine parameters at LEP2, using the simple approximation that 50 CP-even events are sufficient for detection of

a state. Points above the line correspond to states which could be seen, those below to those which could not be seen. The three lines $\sqrt{s} = 175\text{GeV}$, $\int \mathcal{L} = 150\text{pb}^{-1}$ per experiment; $\sqrt{s} = 192\text{GeV}$, $\int \mathcal{L} = 150\text{pb}^{-1}$ per experiment; $\sqrt{s} = 205\text{GeV}$, $\int \mathcal{L} = 300\text{pb}^{-1}$ per experiment; reading from left to right.

Figure 5: Contours of values of Λ_{min} , the value of Λ which can be excluded, in the \sqrt{s} –luminosity plane, labelled in GeV. This is total luminosity, not luminosity per experiment.

Figure 6: $m'_A - \tan\beta$ plane with $\sqrt{s}=175\text{GeV}$, $\int \mathcal{L} = 150\text{pb}^{-1}$ per experiment, $\lambda = 0$, $m_t = 175\text{GeV}$, and squarks degenerate at 1TeV. The dot-dashed line is the kinematic limit for charged Higgs discovery. The dashed lines represent $Z \rightarrow hA$ contours with no singlet mixing (right, corresponding to the MSSM) and worst case mixing (left). The three solid lines show $Z \rightarrow Zh$ contours, derived by assuming no singlet mixing (upper, corresponding to the MSSM), the full scan approach (middle) and the exclusion limit on Λ (lower).

Figure 7: $m'_A - \tan\beta$ plane with $\sqrt{s}=192\text{GeV}$, $\int \mathcal{L} = 150\text{pb}^{-1}$ per experiment, $\lambda = 0$, $m_t = 175\text{GeV}$, and squarks degenerate at 1TeV. The dot-dashed line is the kinematic limit for charged Higgs discovery. The dashed lines represent $Z \rightarrow hA$ contours with no singlet mixing (right, corresponding to the MSSM) and worst case mixing (left). The three solid lines show $Z \rightarrow Zh$ contours, derived by assuming no singlet mixing (upper, corresponding to the MSSM), the full scan approach (middle) and the exclusion limit on Λ (lower).

Figure 8: $m'_A - \tan\beta$ plane with $\sqrt{s}=205\text{GeV}$, $\int \mathcal{L} = 300\text{pb}^{-1}$ per experiment, $\lambda = 0$, $m_t = 175\text{GeV}$, and squarks degenerate at 1TeV. The dot-dashed line is the kinematic limit for charged Higgs discovery. The dashed lines represent $Z \rightarrow hA$ contours with no singlet mixing (right, corresponding to the MSSM) and worst case mixing (left). The three solid lines show $Z \rightarrow Zh$ contours, derived by assuming no

singlet mixing (upper, corresponding to the MSSM), the full scan approach (middle) and the exclusion limit on Λ (lower).

Figure 9: $m'_A - \tan\beta$ plane with $\sqrt{s}=192\text{GeV}$, $f\mathcal{L} = 150\text{pb}^{-1}$ per experiment, $\lambda = 0.5$, $m_t = 175\text{GeV}$, and squarks degenerate at 1TeV. The dot-dashed line is the kinematic limit for charged Higgs discovery. The dashed lines represent $Z \rightarrow hA$ contours with no singlet mixing (right) and worst case mixing (left). The solid line shows the $Z \rightarrow Zh$ contours derived by assuming no mixing. The full scan approach and using the limit on Λ do not allow any part of the plane to be excluded.

Figure 1

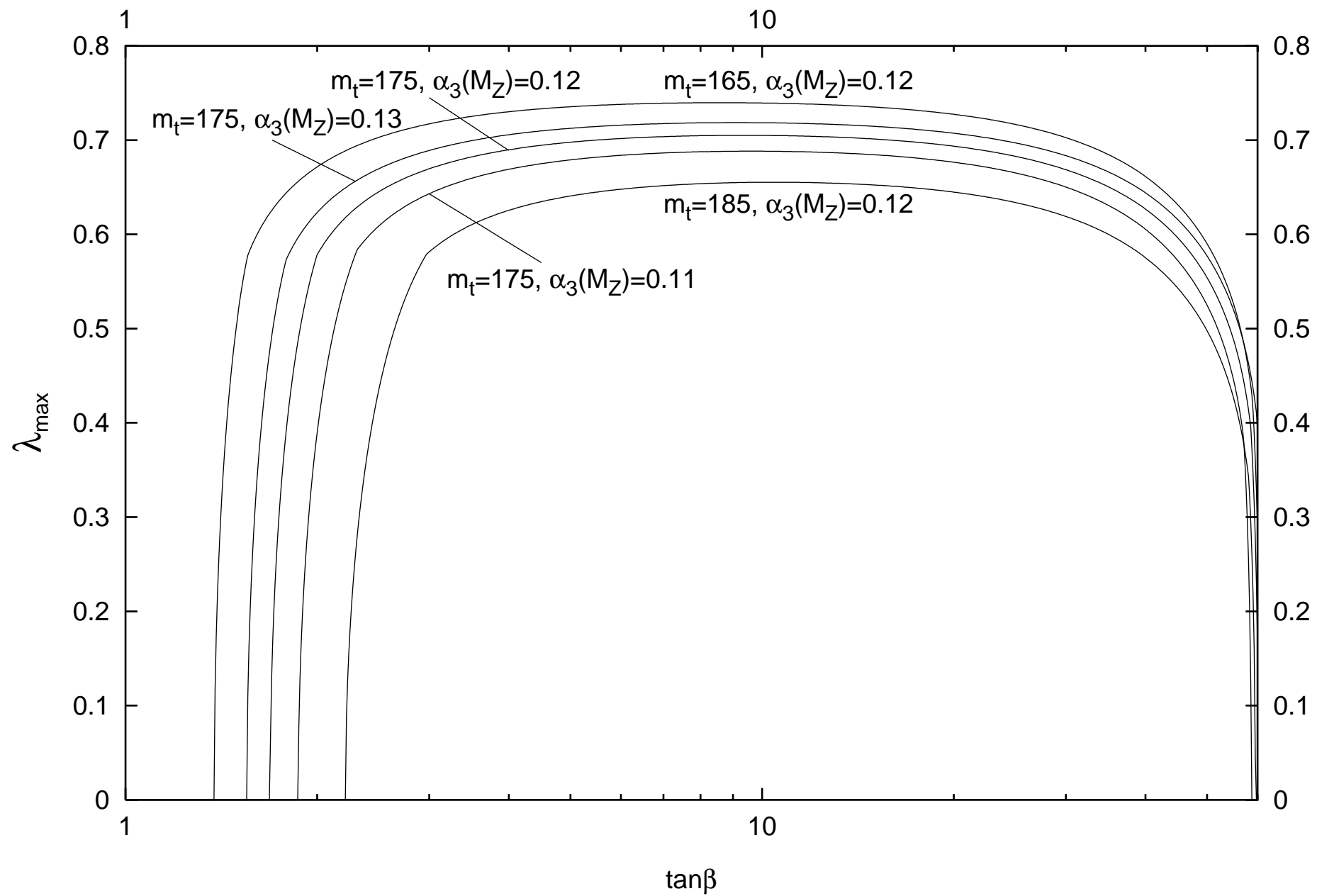


Figure 2

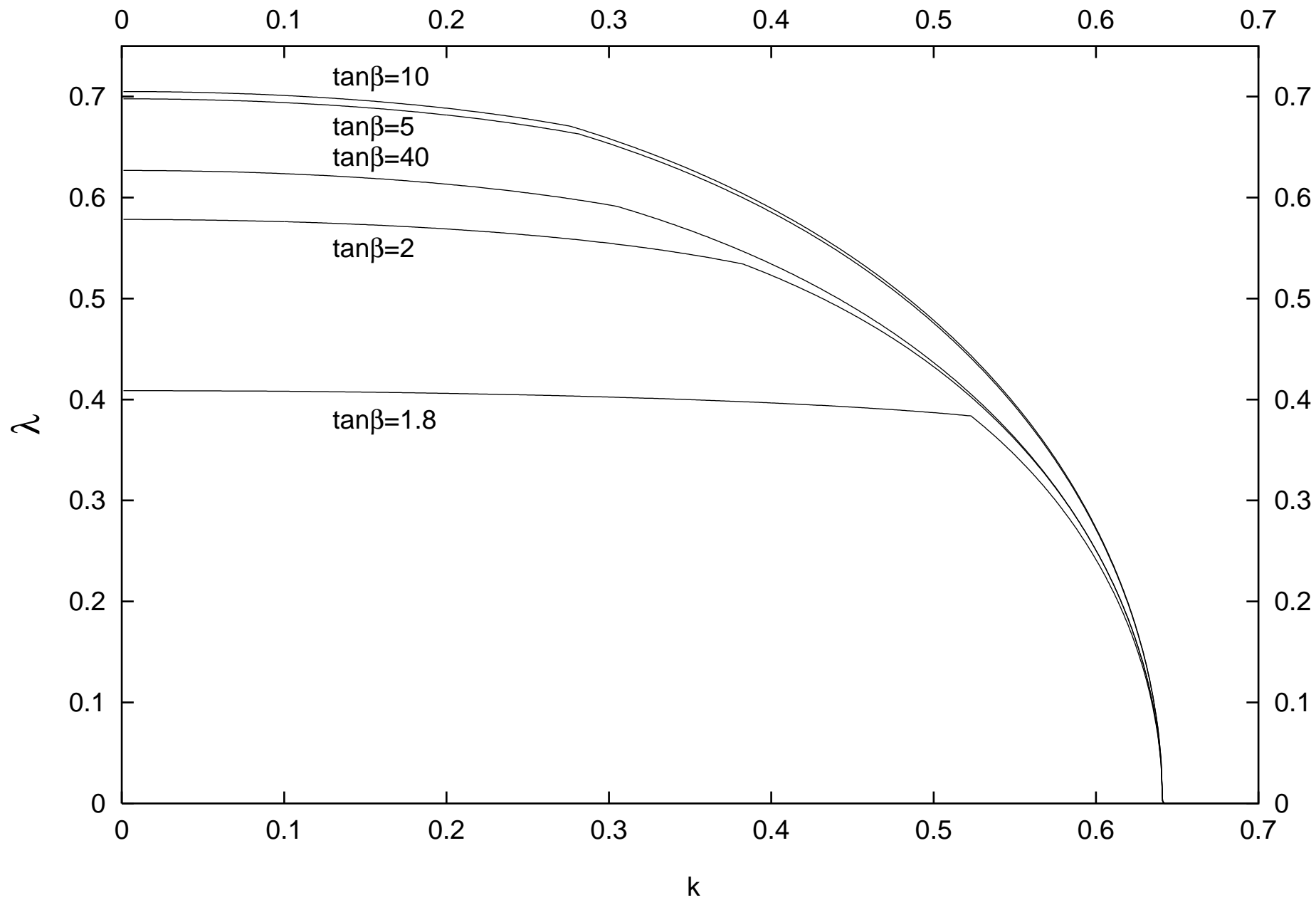


Figure 3a

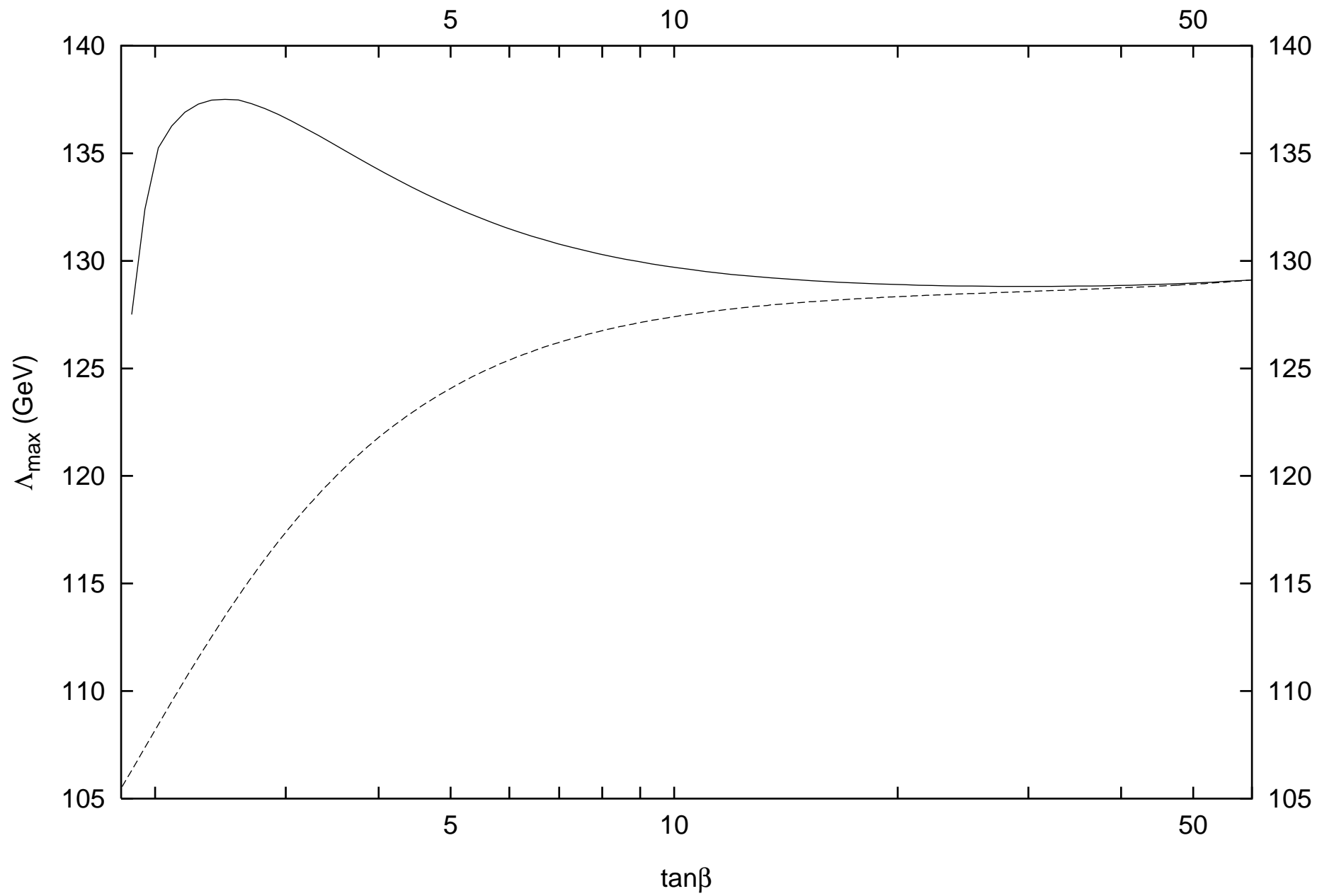


Figure 3b

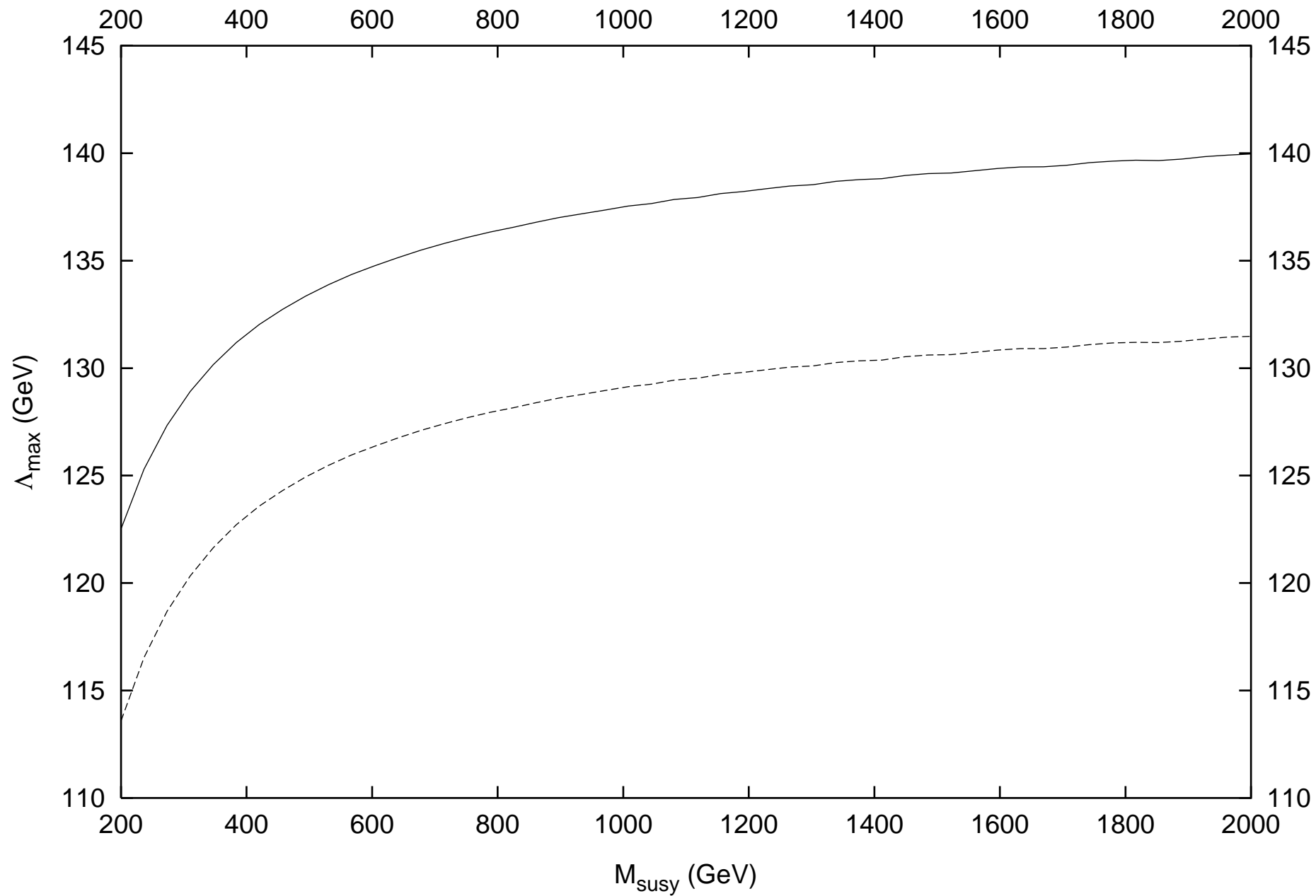


Figure 3c

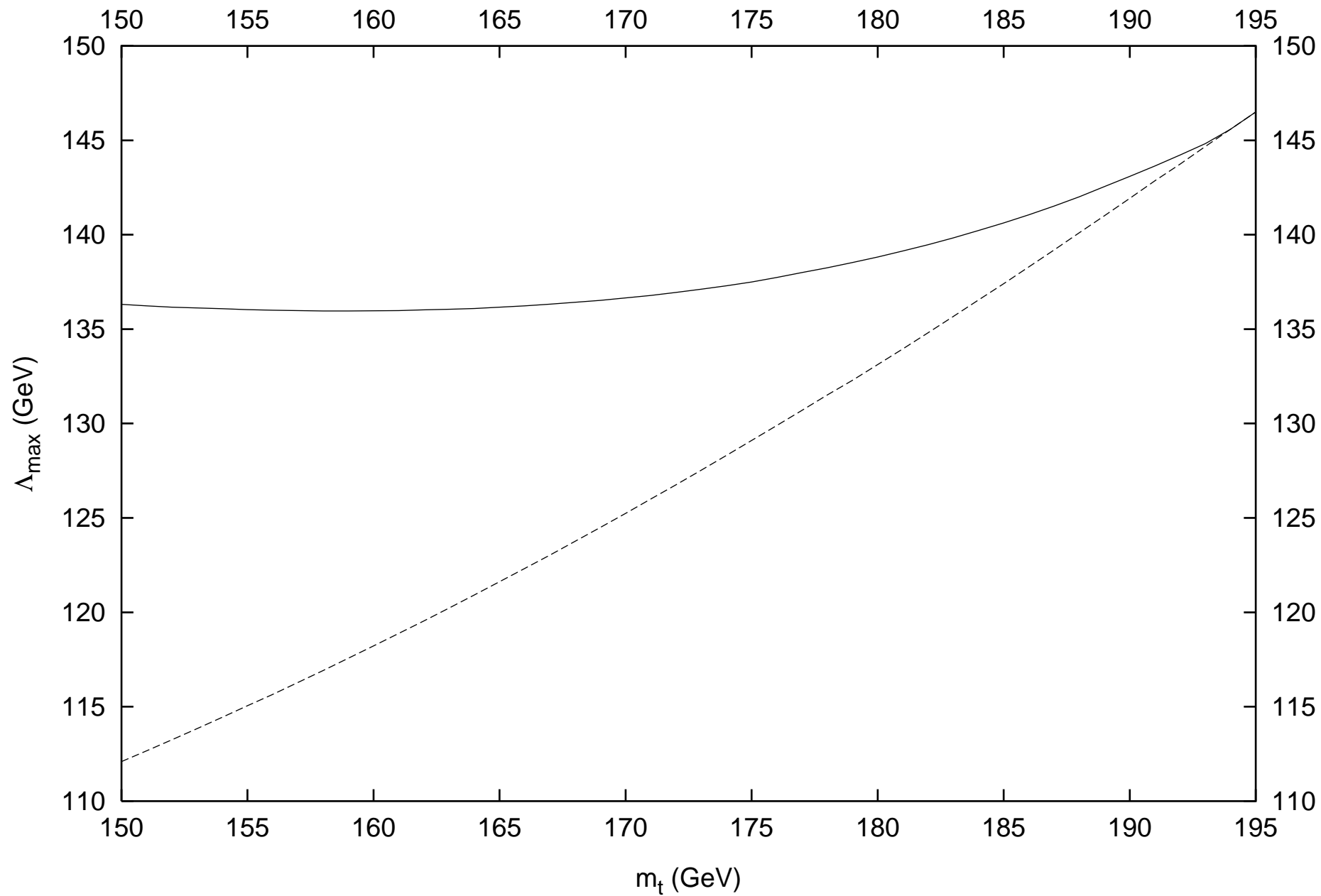


Figure 4a

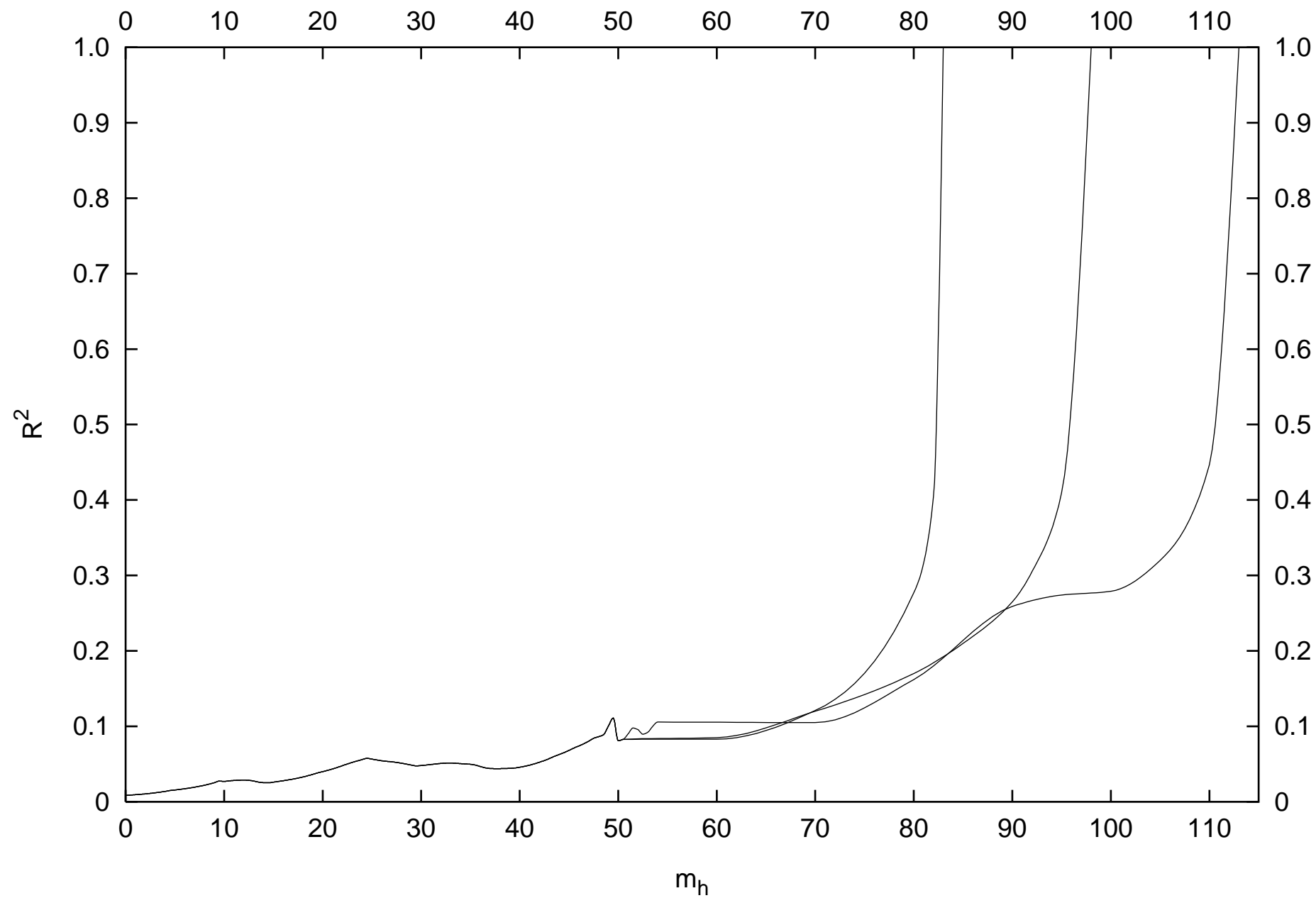


Figure 4b

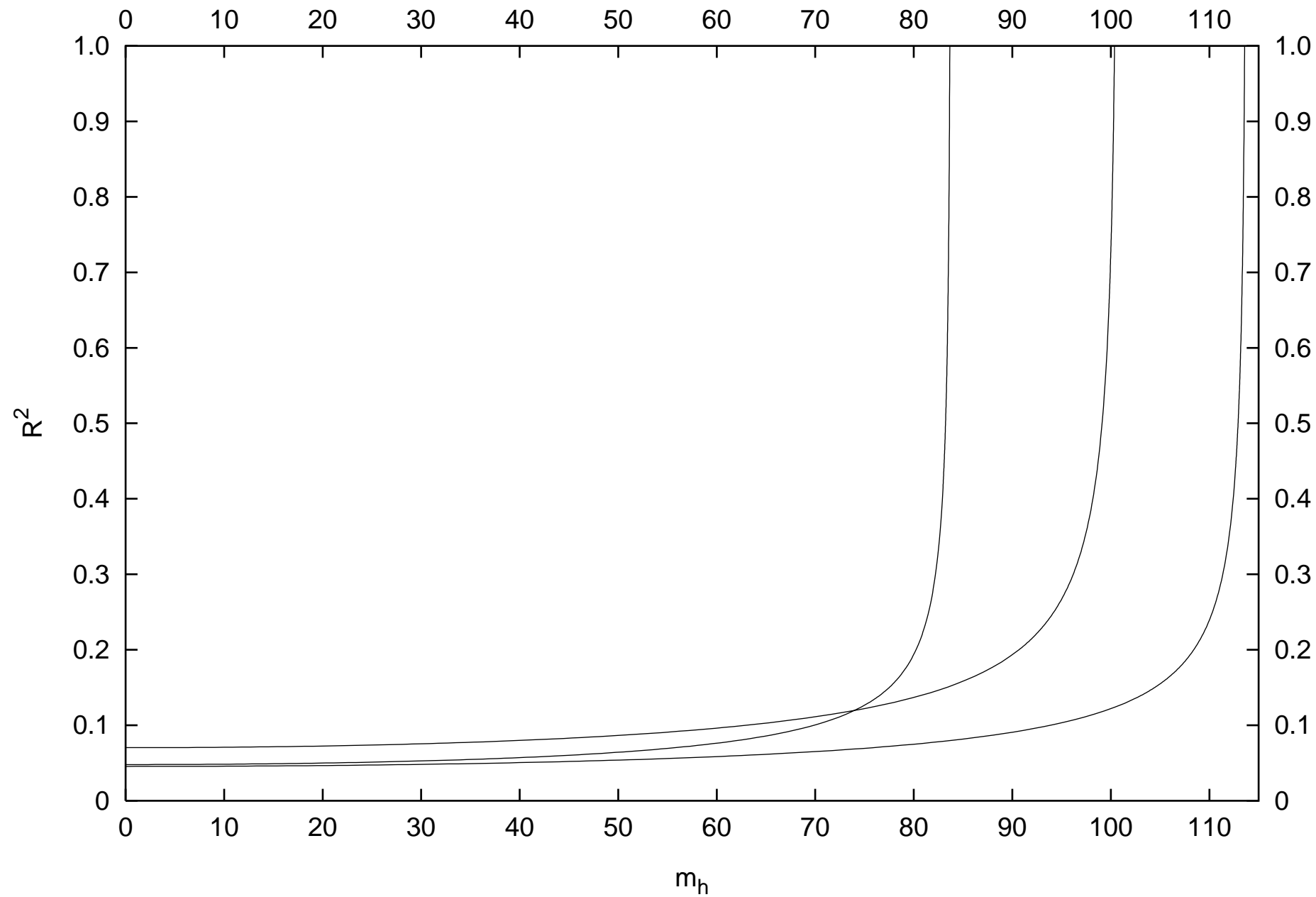


Figure 5

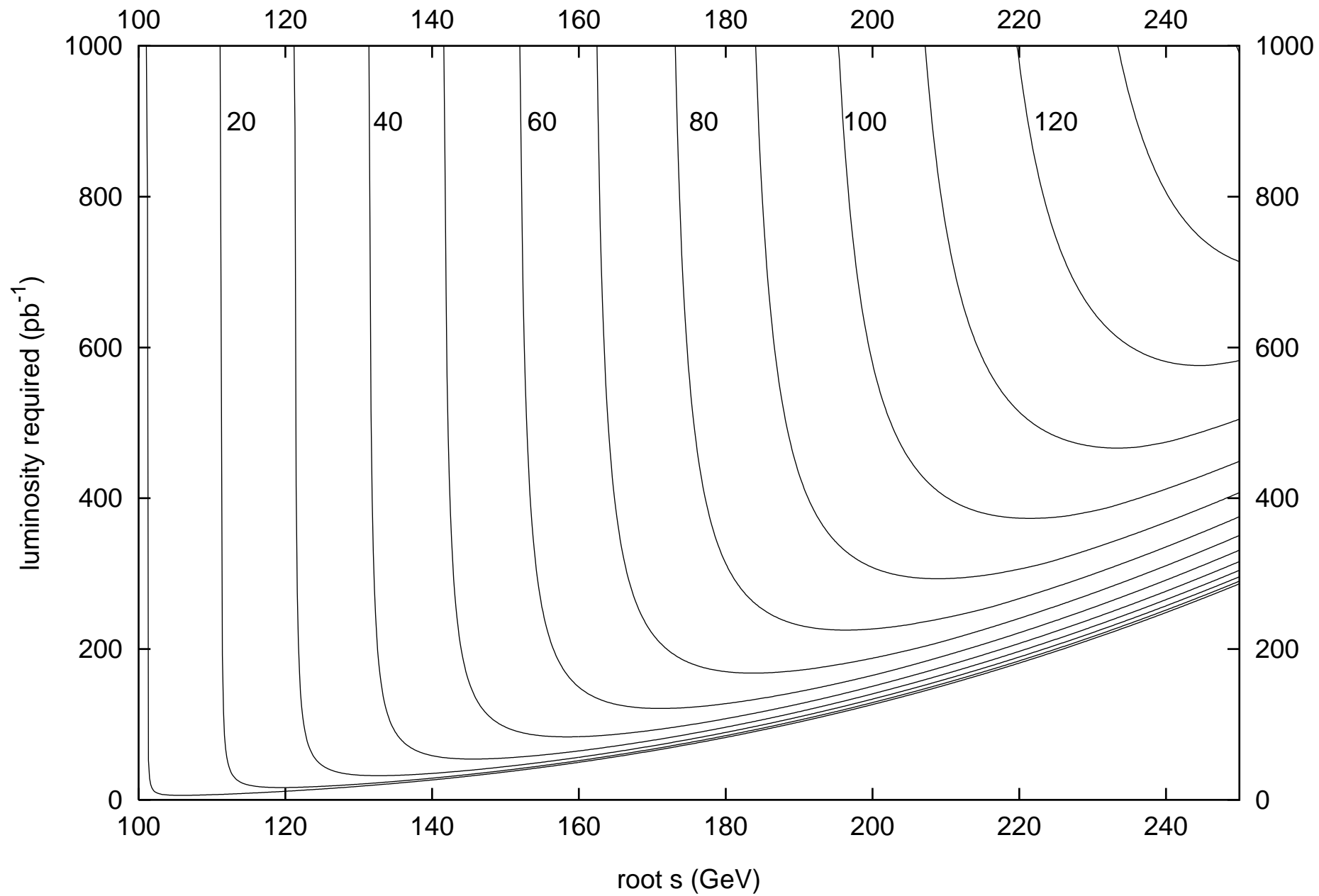


Figure 6

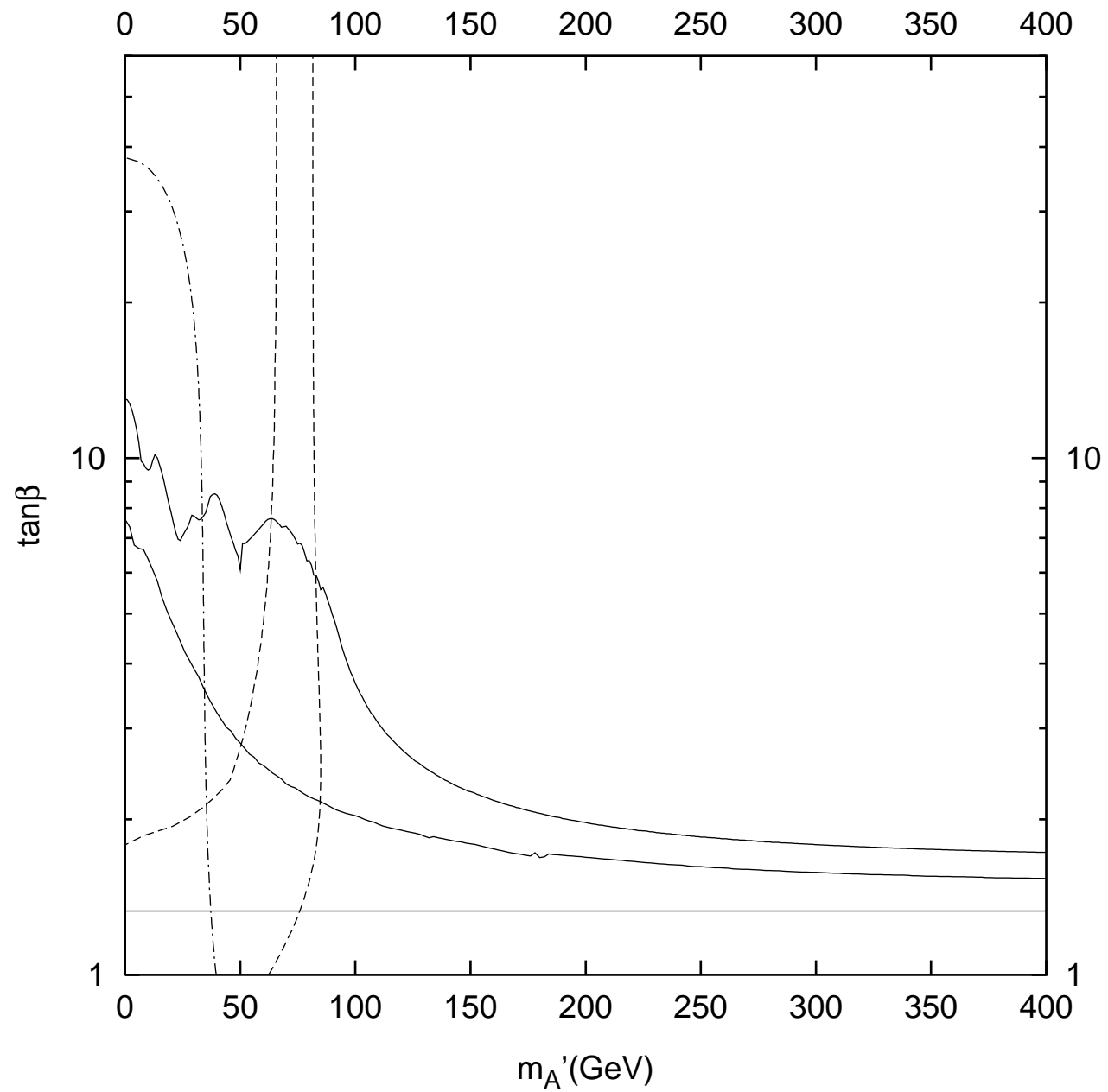


Figure 7

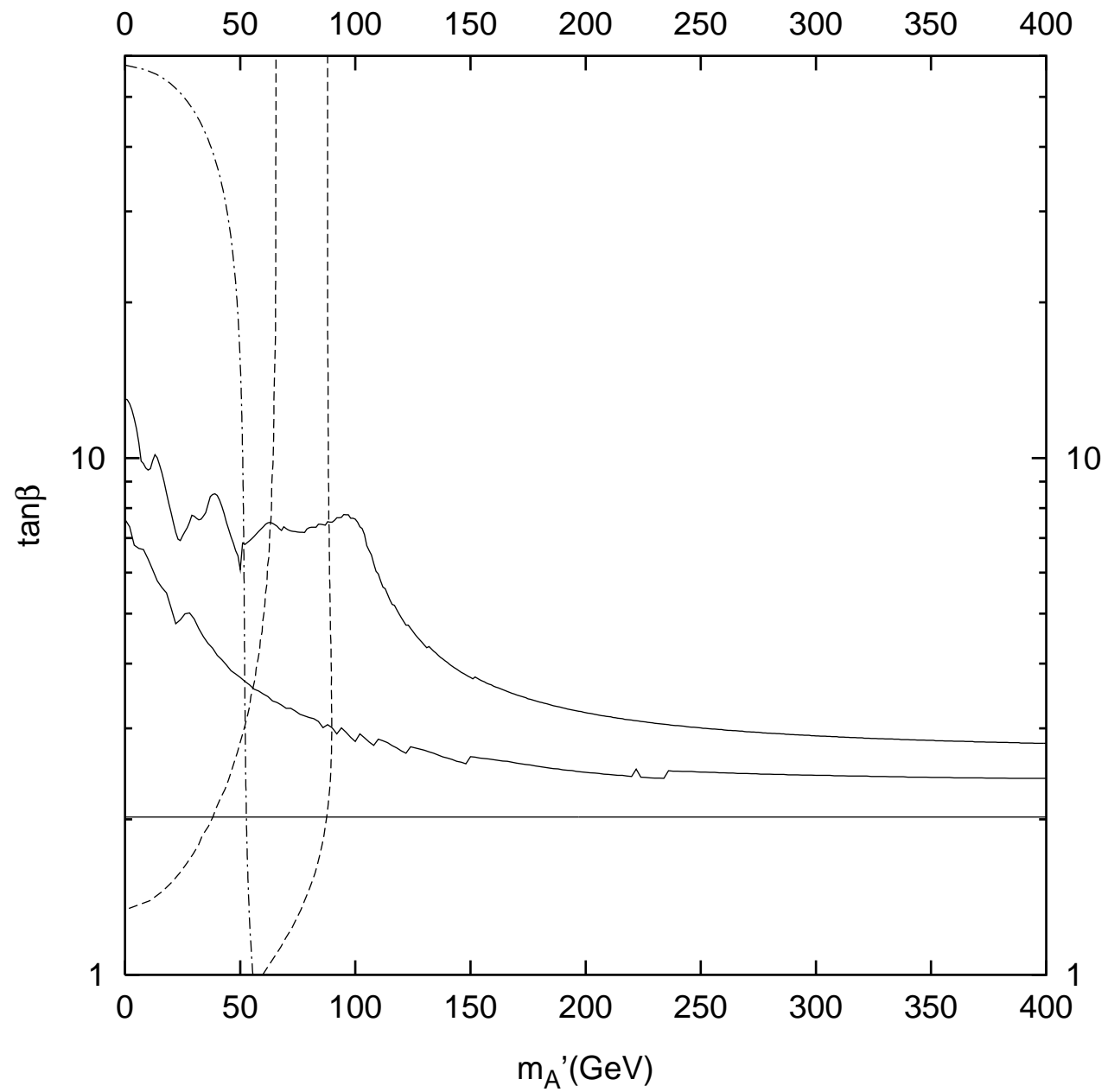


Figure 8

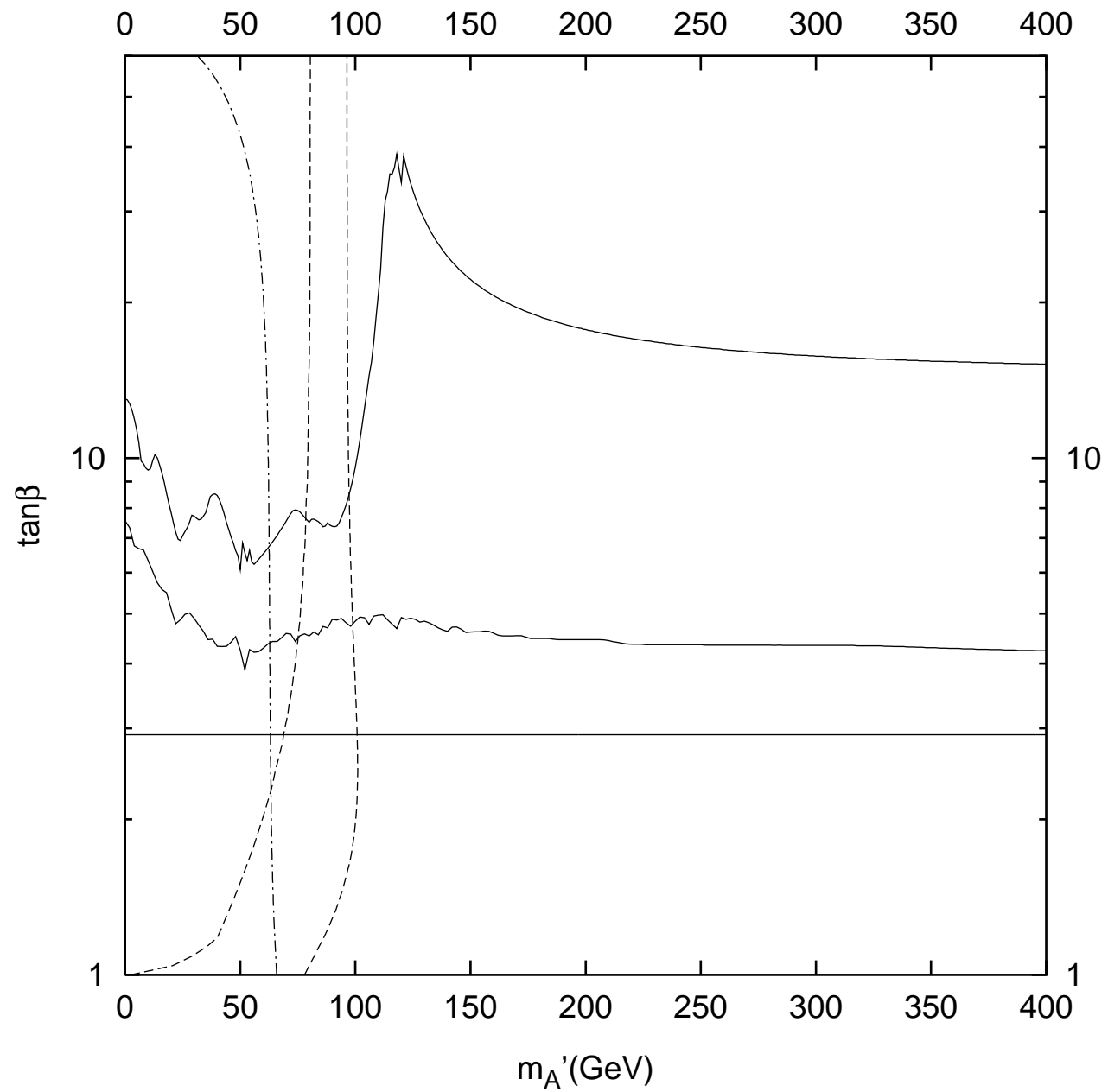


Figure 9

